A method for rapid gain-of-function studies in the mouse embryonic nervous system

Nicholas Gaiano[1,2], Jhumku D. Kohtz[1,2,3], Daniel H. Turnbull[2,4] and Gord Fishell[1,2]

[1] *Developmental Genetics Program and the Department of Cell Biology, New York University School of Medicine, 540 First Avenue, New York, New York 10016, USA*

[2] *The Skirball Institute of Biomolecular Medicine, New York University School of Medicine, 540 First Avenue, New York, New York 10016, USA*

[3] *Present address: Program in Neurobiology, Children's Memorial Hospital, CMIER, Chicago, Illinois 60614, USA*

[4] *Departments of Radiology and Pathology, New York University School of Medicine, 540 First Avenue, New York, New York 10016, USA*

Correspondence should be addressed to either G.F. (fishell@saturn.med.nyu.edu) or D.H.T. (turnbull@saturn.med.nyu.edu)

We used ultrasound image-guided injections of high-titer retroviral vectors to obtain widespread introduction of genes into the mouse nervous system *in utero* as early as embryonic day 8.5 (E8.5). The vectors used included internal promoters that substantially improved proviral gene expression in the ventricular zone of the brain. To demonstrate the utility of this system, we extended our previous work *in vitro* by infecting the telencephalon *in vivo* as early as E8.5 with a virus expressing Sonic Hedgehog. Infected embryos showed gross morphological brain defects, as well as ectopic expression of ventral telencephalic markers characteristic of either the medial or lateral ganglionic eminences.

Genetic analyses of both vertebrates and invertebrates have been critical to advancing our understanding of neural development. Large-scale mutageneses in flies, worms and, more recently, zebrafish have provided an abundance of loss-of-function mutations that have greatly facilitated the study of developmentally interesting genes.

An essential complement to loss-of-function studies are gain-of-function analyses that examine the effects of expressing genes of interest in atypical spatial and temporal patterns. In non-mammalian vertebrates, gain-of-function studies are routinely performed using a variety of approaches. These include the injection of RNA or DNA into early frog and fish embryos[1–3], the infection of chick embryos with retroviral vectors[4], and more recently the electroporation of chick embryos[5]. Gain-of-function work in these systems has been extremely informative, although the lack of mutants, particularly in frogs and chicks, often makes it impossible to fortify conclusions with loss-of-function data.

In mice, gain-of-function studies are more difficult. Such studies are typically performed using viral vectors or transgenes to drive the expression of exogenous genes. These gene delivery systems have limited utility, however, because viral vectors can be cumbersome and/or inefficient, whereas transgenes are costly and require the identification of regulatory elements with specific spatial and temporal patterns. A rapid gain-of-function expression system in the mouse, together with the many mutations currently available, would provide a powerful approach for dissecting genetic pathways in this vertebrate.

Adenoviral and retroviral vectors have been used for gain-of-function studies in mice. Adenoviral vectors can be prepared to extremely high titers and can infect nondividing cells, allowing introduction of genes into postmitotic cells such as neurons[6,7]. However, adenoviral vectors are not ideal for studies examining the role of a given gene in progenitor cells, as infection of postmitotic cells can confound analysis. This issue limits studies of cell-fate specification, because the infection of postmitotic cells, which have already been specified, cannot be distinguished from the infection of progenitors, which are not. In addition, because adenoviral vectors do not integrate into the host genome, they do not stably mark infected cells, complicating the correlation of phenotype with exogenous gene expression.

In contrast, although retroviral vectors are typically much lower titer than adenoviral vectors, retroviruses only infect mitotically active cells and provide stable genetic markers[8–10]. Retroviral marking is used extensively for lineage studies in rodents because these studies require stable infection and low titers[8,9,11–13]. In addition, a handful of gain-of-function studies have been carried out in rodents using retroviruses[14–17]. In general, however, the utility of such studies is limited by low numbers of infections.

Here we describe a rapid gain-of-function gene expression system for use in mice *in utero*. We used methods that permit routine production of retroviral vectors to titers ranging from 1×10^8 to 5×10^9 cfu per ml. These vectors are 'pseudotyped', containing murine leukemia virus (MLV)-based genomes and the vesicular stomatitis virus (VSV) envelope. Furthermore, we found that vectors including an enhancer/promoter located downstream of the 5′ long terminal repeat (LTR) are much more effectively expressed in the ventricular zone (VZ) of the brain than those using the LTR to drive gene expression.

To infect developing mouse embryos with these viruses, we used an ultrasound backscatter microscopy (UBM) system that permits real-time visualization and injection of embryos *in utero*[18,19]. We injected retroviral stocks into embryos as early as E8.5, a time at which the neural plate is open in much of the brain and spinal cord. Infection at this time permits introduction of genes along the rostrocaudal extent of the neuraxis during early neural patterning and cell-fate specification.

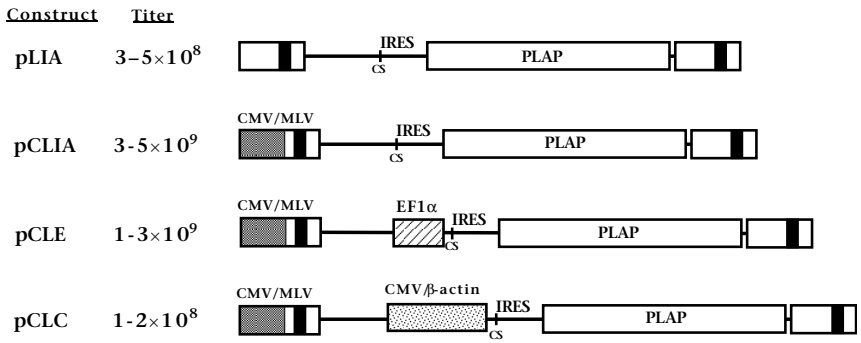

Fig. 1. Schematic representations of the retroviral constructs. pCLIA was made by replacing the 5′-LTR of pLIA[17] with that of the pCL vector, which includes the CMV regulatory sequence[21]. Either the *Xenopus* EF1α or the CMV/chicken β-actin regulatory elements was inserted upstream of the internal ribosome entry sequence (IRES) to make pCLE and pCLC. The IRES sequence permits translation of the second cistron containing the reporter gene human placental alkaline phosphatase (PLAP). The titer range obtained when making MLV/VSV stocks of each construct is indicated. cs, cloning site.

We used this method to extend our previous *in vitro* studies investigating the role of Sonic Hedgehog (Shh) in telencephalic development[20]. In doing so, we found that ectopic clusters of Shh-expressing cells located laterally or dorsally in the telencephalon *in vivo* could induce the expression of ventral markers characteristic of either the medial or lateral ganglionic eminences (MGE and LGE).

Results

Comparison of pseudotyped with ecotropic vectors

The primary limitation of retroviral vectors for gain-of-function studies in mice has been difficulty in obtaining high-titer stocks. Therefore, we used the CMV enhancer/promoter to drive virus production in the packaging cells. This modification does not affect proviral LTR structure and increases viral titer[21]. Consistent with previous work, we obtained a tenfold increase in titer when using constructs differing only in design of the 5′-LTR (**Fig. 1**).

To further increase viral titers, we used pseudotyped vectors that included MLV-based core particles and the envelope glycoprotein (G) of VSV[22]. Such viruses are essentially hybrids with the internal components of the MLV-based retrovirus and the external envelope of the VSV rhabdovirus. As a result, cell penetration is mediated via the VSV envelope, but upon penetration the retroviral RNA genome is reverse transcribed into proviral DNA and integrated into the target cell's genome. The primary advantage of this type of vector is that, unlike more standard murine vectors, which use the rodent-specific ecotropic or broader-spectrum amphotropic envelopes, it can be concentrated by ultracentrifugation without a substantial loss of infectivity[22].

The broad host range of VSV is thought to be the result of the virus utilizing a membrane phospholipid as a receptor to permit cell penetration[23]. In contrast, MLV uses a transmembrane protein as a receptor and has a much more limited host range[24]. Based upon the ubiquitous nature of the VSV receptor, we believed that MLV/VSV vectors would be capable of penetrating most cells in the developing embryo. To compare MLV/VSV vectors to the more commonly used ecotropic viruses, we injected the telencephalon of E9.5 embryos with either CLIA(G) (virus pseudotyped with the VSV-G protein) or CLIA(E) (virus with the ecotropic envelope) and compared the percentage of labeled cortical neurons at postnatal day 21 (P21). Embryos were visualized for injection using a previously described ultrasound-imaging system[18,19]. The sole purpose of this system was to visualize the embryo and guide the injection, and no mechanical effects on the virus or embryo are expected.

Infected cells were detected by staining for the human placental alkaline phosphatase gene (PLAP) contained in the viral vector (**Fig. 1**). This gene has been widely used because its membrane localization makes it an excellent marker to reveal cell morphology. To confirm that the morphological criteria we were using to identify neurons and glia were accurate, we used double immunofluorescence to detect PLAP together with neuronal or glial markers (**Fig. 2a–l**). Such staining demonstrated that the membrane localization of PLAP permitted cell type identification. Subsequently we used the histochemical substrates BCIP/NBT to determine the identity of infected cells (**Fig. 2m–r**).

At P21, samples infected with ecotropic CLIA(E) had 24.0 ± 6.1% labeled cortical neurons ($n = 4$, 169 neurons and 542 glia scored in total), whereas samples infected with pseudotyped CLIA(G) had 39.3 ± 2.9% labeled cortical neurons ($n = 4$, 638 neurons and 977 glia scored in total; **Fig. 2s**). This difference suggests that one of the viral envelopes, if not both, may recognize heterogeneity among E9.5 neocortical progenitors. For example, such heterogeneity might be in the form of differential expression of the ecotropic receptor. Additional studies will be needed to explore this point. Nonetheless, the finding that pseudotyped virus labeled a higher percentage of neurons than ecotropic virus is fortuitous for those interested in studying neurons.

Internal promoters improve expression in the VZ

In the past, most studies with retroviral vectors in the mammalian brain used vectors that drive gene expression from the MLV LTR. Although this promoter drives strong gene expression in numerous different cell types, it is silenced in cells possessing stem cell characteristics, such as embryonic carcinoma cells, embryonic stem cells and hematopoeitic stem cells[25–27]. A variety of studies suggest that neural stem cells may exist in mammals[28–30], raising the possibility that the MLV LTR might be silenced in these as well. Furthermore, vectors using the MLV LTR to drive gene expression seem to be silenced in neurons of the mature striatum[31].

We were concerned about the possibility of retroviral silencing because the telencephalon is a single cell layer at the stages we infected, and many telencephalic progenitors are likely to have stem-cell properties. Preliminary data from our *in vivo* lineage studies using the LTR to drive reporter expression supported the notion that significant silencing occurs. Based on reported expression, most clones labeled at E9.5 appeared to be single cells (M. McCarthy, D. H. T. and G. F., unpublished data). This was surprising, given the finding that, at E9.5, most precursors undergo symmetric divisions to expand the progenitor pool[32] and would therefore be expected to give rise to many daughter cells later in development.

To address the possibility of LTR silencing, we compared pCLIA, which used the MLV LTR to drive gene expression, and two additional constructs, pCLE and pCLC, which contained

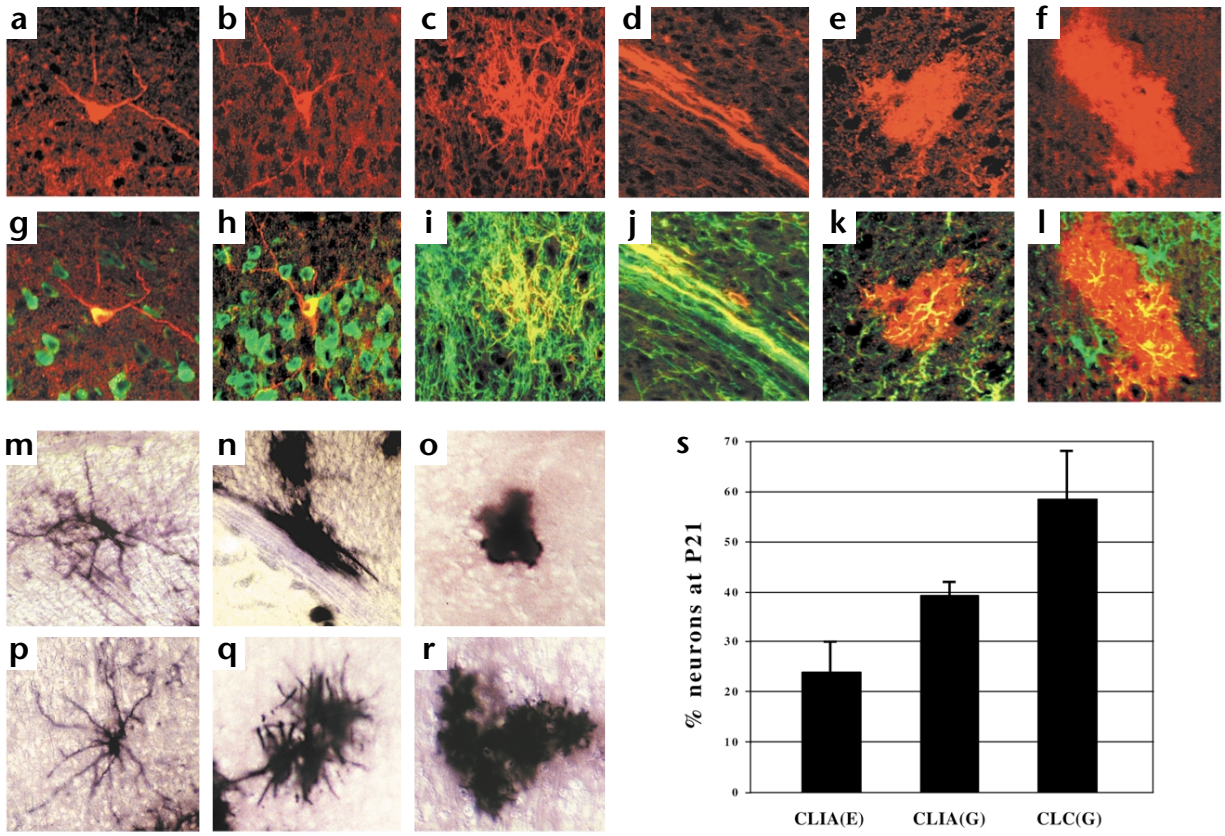

Fig. 2. P21 phenotype of cells infected with PLAP-expressing viruses at E9.5. **(a–f)** P21 cells infected with CLIA(G), identified using an antibody that recognizes PLAP. Morphologies suggestive of neurons **(a, b)**, oligodendrocytes **(c, d)** and astrocytes **(e, f)** are evident. To confirm the identity of these cells, they were double labeled with a neuronal marker, NeuN[48] **(g, h)**, an oligodendrocyte marker, CNPase[49] **(i, j)** or an astrocyte marker, GFAP[50] **(k, l)**. Yellow indicates colocalization of these markers with PLAP. Samples stained with BCIP/NBT to reveal the morphology of infected cells **(m–r)**, were used to score cell types. Neuronal **(m, p)**, oligodendroglial **(n, q)** and astroglial **(o, r)** morphologies were seen. **(s)** Histogram comparing the percentage of labeled neurons scored at P21 in the neocortex of samples infected with CLIA(E), CLIA(G) and CLC(G). In each case, 4 samples were sectioned on a cryostat at 30 μm, and every sixth section was scored. To roughly correct for scoring glia as large, darkly stained objects (30–50 μm), while scoring neurons only when the cell body was evident (10–15 μm), the number of glia scored was divided by three. Standard deviation is shown.

internal transcriptional regulatory sequences (**Fig. 1**). The *Xenopus* elongation factor-1α enhancer/promoter (EF1α) is contained in pCLE[33], and the CMV enhancer and the promoter of the chicken β-actin gene (together referred to as CA) is included in pCLC[34,35]. Embryos injected at E9.5, with each of these viruses were sacrificed at E14.5, and the distribution of PLAP+ cells was evaluated. The injection of 4×10^9 cfu per ml CLIA(G) resulted in very widespread infection (**Fig. 3a** and **b**). However, the labeled cells were not distributed evenly throughout the tissue and, in particular, were severely underrepresented in the VZ ($n = 17$ embryos). This result suggests that CLIA is either silenced or very weakly expressed in the VZ. In contrast, embryos injected with 4×10^8 to 2×10^9 cfu per ml CLE(G) showed widespread infection in both the ventricular and postmitotic zones ($n = 11$ embryos; **Fig. 3c** and **d**). It is noteworthy, however, that without the nested promoter, silencing in the VZ was not absolute. CLIA(G)-infected samples typically had a limited number of PLAP+ cells in the VZ, found as either individual cells or dense clusters (arrowheads in **Fig. 3a**). In samples infected with lower titers of CLIA(G), isolated clusters that spanned the distance from ventricular to pial surfaces could be found (data not shown). Nevertheless, as shown in Fig. 3, a typical example of high-titer infections, the majority of telencephalic tissue infected with CLIA(G) seemed to show silencing in the VZ.

Thus the MLV LTR did not drive high levels of expression in all cells, and the EF1α promoter increased the proportion of infected cells that expressed PLAP at detectable levels. Although the lower titers obtained with CLC(G) precluded infection levels obtained with CLIA(G) and CLE(G), the distribution of labeled cells in CLC(G)-infected samples suggest that this virus also labeled the VZ more effectively than CLIA(G). In the neocortex, for example, most CLC(G)-infected clusters reached from the ventricular to the pial surfaces (**Fig. 3e–g**), indicating that this construct was expressed well in both ventricular and postmitotic cells.

To further compare reporter expression from these viruses, we examined samples infected at E9.5 and killed at P21. The most striking contrast was between CLIA and CLC. In CLIA(G)-infected samples, individual cortical neurons were usually spatially isolated from one another (**Fig. 4a**). In CLC(G)-infected samples, however, cortical neurons were often found in large, radial clusters, consistent with the radial migratory path taken by newborn

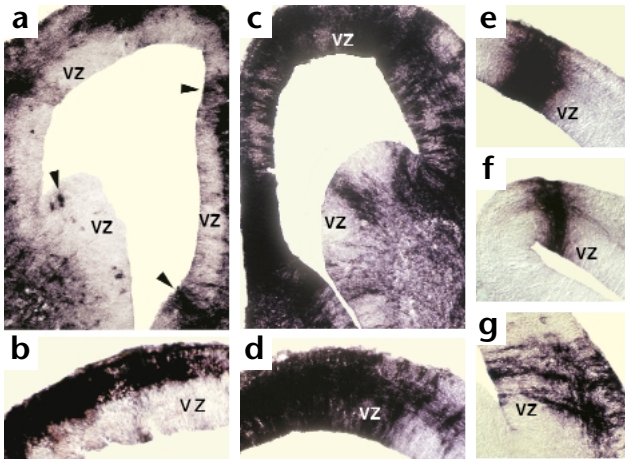

Fig. 3. Internal promoters improved vector expression within the ventricular zone. In all cases, samples were injected at E9.5 and killed at E14.5. **(a, b)** Samples infected with 4×10^9 cfu per ml CLIA(G). Although the postmitotic areas were heavily labeled, the ventricular zone (VZ) was not. However, some clusters of stained cells could be found in the VZ (arrowheads). **(c, d)** Samples infected with 2×10^9 cfu per ml CLE(G) were heavily labeled in both the VZ and postmitotic area. **(e–g)** Samples infected with 1×10^8 cfu per ml CLC(G) had clusters of labeled cells spanning from the ventricular to pial surfaces.

cortical neurons (**Fig. 4b**)[36,37]. Another noteworthy difference between CLIA and CLC was that, whereas labeled striatal neurons were rarely found in CLIA(G)-infected samples, they were common in CLC(G)-infected samples (**Fig. 4c**). At P21, CLE(G)-infected samples resembled those infected with CLC(G), although the labeled neurons were generally more weakly stained.

To determine whether the percentage of labeled neurons in CLC(G)-infected brains differed from that of CLIA(G)-infected brains, we scored neurons and glia at P21 as described above. Whereas $39.3 \pm 2.9\%$ of the labeled cells were neurons in CLIA(G)-infected samples (see above), $58.3 \pm 9.7\%$ were neurons in CLC(G)-infected samples ($n = 4$, 1120 neurons and 717 glia scored in total; **Fig. 2s**). The finding that inclusion of the CA regulatory element increased the fraction of labeled neurons suggests that silencing of the LTR was more prevalent in neurons. This observation is consistent with the roughly four- to fivefold greater abundance of labeled striatal neurons seen in the CLC(G)-infected samples than in CLIA(G)-infected samples (data not shown).

Widespread infection of E8.5 embryos *in utero*

Although the UBM system can be used to inject E9.5 mouse embryos[19], we wanted to inject even earlier. Injection at E9.5 is not optimal for gain-of-function studies addressing early patterning events in the brain and spinal cord. Although portions of these structures are probably still being patterned at this age, retroviral vectors do not express their gene products until 12–24 hours after initial infection. Therefore, injection at E9.5, which results in expression by E10.0–E10.5, is likely to be too late for many ectopically expressed genes to influence patterning. Injections a day earlier, at E8.5, offer the advantage that the brain and spinal cord are still largely open to the amnionic fluid.

We first injected CLE(G) into E8.5 embryos to assess survival after surgery *in utero* at this age, as well as the extent of retroviral infection (**Fig. 5**). Of 54 embryos injected with CLE(G), 22 survived to E12.5 (41%). Of these, nine had exencephaly (open forebrain), although the trunk appeared morphologically normal. The cause of the exencephaly is unknown, although it seemed to be a consequence of injection into the E8.5 amnion. Infected embryos were sectioned and stained to detect PLAP+ cells, and both the brain and spinal cord were found to be heavily infected (**Fig. 5d, e, g** and **h**). Infection in the brain was extensive and included forebrain, midbrain and hindbrain structures. In the spinal cord, infection was found at all dorsoventral positions, including the floor plate. Furthermore, many infected cells were seen in the dorsal root ganglia (**Fig. 5f**). In addition to neural structures, infected cells were also detected in the limbs, gut, liver, heart and other tissues (data not shown).

Ectopic Sonic Hedgehog causes patterning defects

Our motivation for developing this method stemmed from an interest in using *in vivo* gain-of-function studies to better understand mammalian telencephalic patterning. Our previous *in vitro* results suggest that the telencephalon undergoes temporal changes in its response to Shh[20]. To extend this work, we examined the effects of ectopically expressing *shh* in the developing mouse telencephalon *in vivo*. The complete open reading frame of the human *shh* cDNA was subcloned into pCLE, upstream of the IRES sequence (see **Fig. 1**). Concentrated viral stocks of both CLES(G) (Shh-expressing virus) and CLE(G) (control) were prepared and injected into either the amnionic cavities of E8.5 embryos or the telencephalic ventricles of E9.5 embryos using the UBM system. Embryos were then killed at E12.5, examined for gross morphological defects and sectioned for further analysis.

Although the CLES(G) viral stocks were prepared to titers of $3–7 \times 10^8$ cfu per ml, injection of these titers generally resulted in the death of injected embryos. This toxic effect was likely a function of Shh expression rather than other factors in the concentrated stock, as injection of undiluted control-virus stocks was not as lethal. Consequently, CLES(G) was injected at titers of $5–10 \times 10^7$ cfu per ml.

Embryos infected with CLES(G) at either E8.5 or E9.5 exhibited severe brain malformations (**Fig. 6**). In most cases, the forebrain and midbrain were substantially enlarged compared to embryos injected with control virus (with CLES at E8.5, 31 of 34, at E9.5, 37 of 42; with CLE at E8.5, 0 of 13, at E9.5, 0 of 11). In addition, some embryos injected with CLES(G) had kinked neural tubes and limb defects (data not shown). Coronal sections of infected embryos revealed that the telencephalic ventricles were

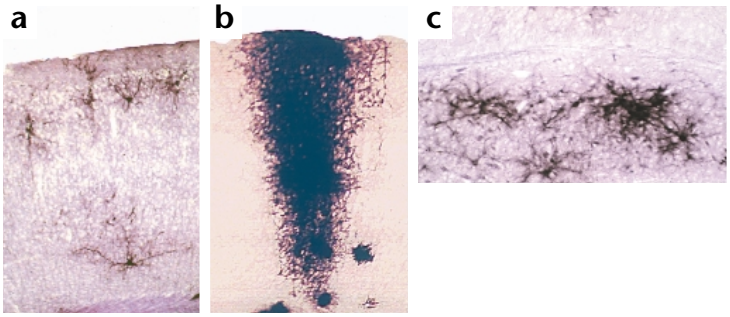

Fig. 4. Comparison of neuron distribution in samples infected with CLIA(G) and CLC(G). **(a)** In CLIA(G)-infected samples, labeled neurons were usually spatially isolated from one another. **(b)** In CLC(G)-infected samples, labeled neurons were often found as large, dense, radial columns. Immunofluorescence staining to detect PLAP more clearly revealed neuronal morphologies within such clusters (not shown). **(c)** Striatal neurons infected with CLC.

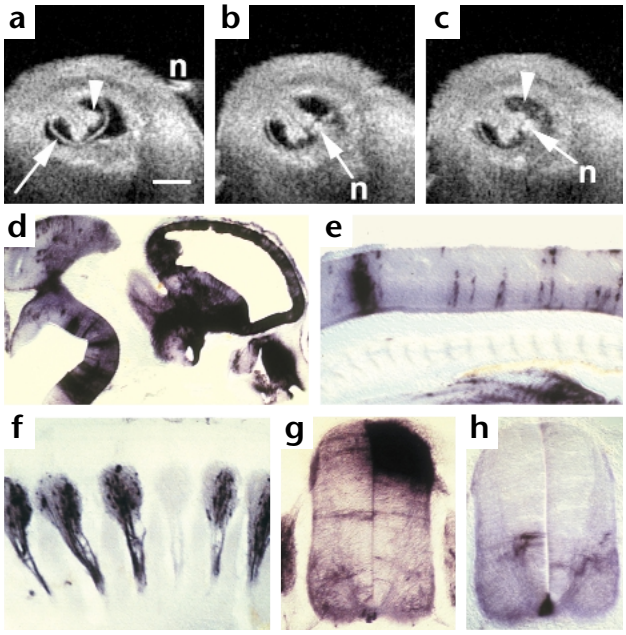

Fig. 5. Injection of retroviral stocks at E8.5 resulted in widespread infection. **(a–c)** UBM images depicting injection into the amnionic sac of an E8.5 embryo. Scale bar, 1 mm. **(a)** The head folds are evident (arrowhead), as is the amnionic membrane (arrow). The needle tip is represented by a bright spot on the screen (n). **(b)** The needle has penetrated the uterus and amnionic sac. **(c)** During injection, the viral stock could be seen filling the amnionic cavity (arrowhead). Infected cells were found throughout the brain **(d)** and spinal cord **(e, g, h)** of E12.5 embryos. In addition, many dorsal root ganglia contained labeled cells **(f)**.

greatly expanded, often into a single ventricle, with an apparent loss of dorsal midline structures such as the hippocampus and choroid plexus (data not shown). Furthermore, in some cases, tissue thickening was associated with CLES infection sites (**Fig. 6b**).

In light of the well-documented role of Shh in dorsal–ventral patterning of the nervous system[38–40], we chose to examine expression patterns of several markers of ventral telencephalic identity in CLES(G)-infected samples. We showed previously that Shh can ventralize dorsolateral telencephalic tissue in culture[20]. To extend these studies, we performed *in situ* hybridization on brains infected with CLES at E9.5 using an antisense riboprobe against *dlx2*, a gene expressed ventrally in both the MGE and LGE, but not dorsally in the neocortex[41]. Expression of CLES in the dorsal telencephalon induced the expression of *dlx2* (**Fig. 7a–d**). In contrast, samples infected similarly with CLE control virus did not express *dlx2* dorsally (data not shown).

To further characterize the ventralizing effect of Shh in the developing telencephalon, we tested for induction of markers specific to either the MGE or LGE. Antibodies recognizing either Nkx2.1 or cellular retinoid binding protein I (CRBP) were used to stain E12.5 samples infected with CLES(G) at E8.5. Nkx2.1 is expressed in the MGE but not the LGE or cortex[20,42], and its expression can be induced *in vitro* by Shh protein[20,43]. At E12.5, CRBP is expressed in the LGE but not in the MGE or cortex, making it a suitable early marker for LGE identity[44]. Double-immunofluorescence staining revealed induction of both Nkx2.1 and CRBP by Shh in dorsal and lateral telencephalic tissue *in vivo* (**Fig. 7e–k**). Nkx2.1 expression was detected either in cells infected with CLES or in nearby cells, suggesting that these cells adopted an MGE-like identity. Staining for CRBP revealed that Shh could induce an LGE-specific marker as well (**Fig. 7h–k**). Interestingly, although this induction generally occurred in the CLES-infected cells, in one case, CRBP was predominantly induced in tissue immediately adjacent to the CLES-expressing cluster (**Fig. 7k**).

Discussion

Rapid gain-of-function studies in the mouse

Our method allows rapid gain-of-function studies in the developing mouse nervous system. Using this method, genes of interest are prepared as retroviral stocks that can be introduced into mitotically active progenitor populations *in vivo* as early as E8.5 and at all subsequent stages. This temporal versatility simplifies comparisons of the effects of a given gene at various times during development. Furthermore, variation in the site of infection provides a wide range of spatial patterns for analysis. Similar studies using transgenic mice would require a very large number of *cis*-acting regulatory elements. In light of the limited availability of such elements, this requirement is prohibitive.

We chose MLV/VSV pseudotyped retroviral vectors because they could be concentrated to very high titers. The ability to infect large numbers of cells was essential for the success of this gain-of-function approach. Although retroviruses have long been available for gain-of-function studies, the low titers typically attained greatly limited the utility of this approach. In addition, previously used vectors, which generally relied on the LTR to drive gene expression, may have been significantly impaired by silencing.

The silencing we observed came to our attention primarily because we used tools that have only recently become available. First, the ability to perform lineage studies from E9.5 in the mouse, made possible using UBM-guided injections, raised concerns about the very small clone sizes observed from this early developmental stage (M. McCarthy, D.H.T. and G.F., unpublished data). Second, preparation of CLIA(G) to 4×10^9 cfu per ml using the VSV envelope permitted such a high level of infection that the dramatic underrepresentation of vector expression in the telencephalic ventricular zone became obvi-

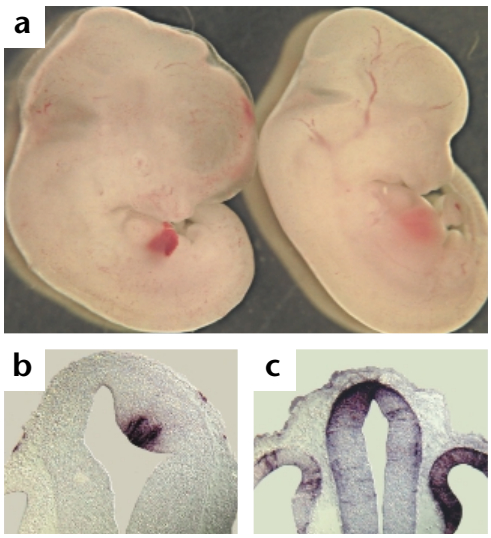

Fig. 6. Morphological defects in embryos infected with a Shh-expressing virus (CLES). **(a)** CLE(G)- and CLES(G)-infected samples (right and left, respectively). Both were injected at E8.5 and killed at E12.5. The CLES(G)-infected embryo had a grossly enlarged head. **(b)** A cluster of CLES-expressing cells in the dorsal diencephalon caused thickening of the adjacent tissue, but this effect was not seen in control CLE samples **(c)**.

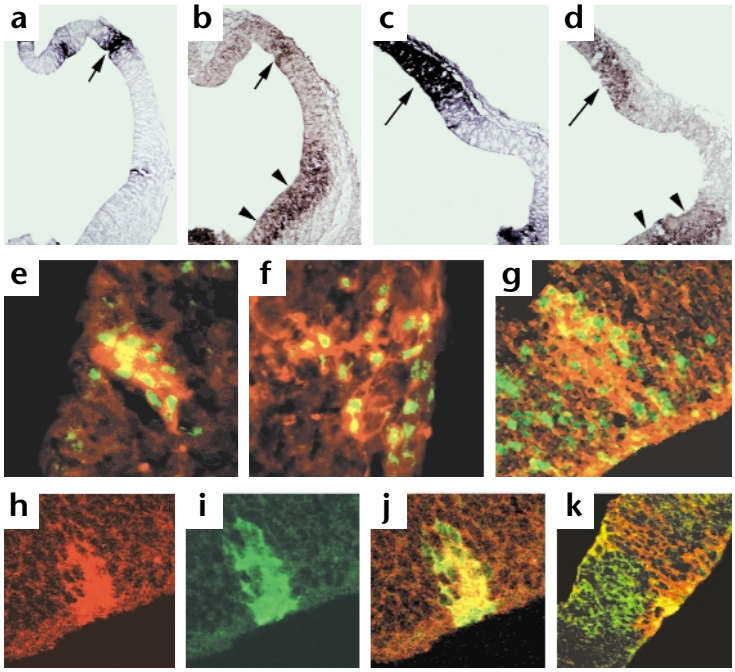

Fig. 7. Dorsolateral Shh expression resulted in ectopic expression of ventral markers. **(a–d)** CLES induces dorsal expression of *dlx2*. **(a, c)** Histochemical staining for PLAP revealed the location of CLES infected cells (arrows). **(b, d)** *In situ* hybridization in adjacent sections reveals that *dlx2* is expressed at the sites of ectopic Shh. The normal ventral expression of *dlx2* was also evident (arrowheads). **(e–g)** Double immunofluorescence labeling to detect PLAP (red) and the MGE-specific marker Nkx2.1 (green) demonstrates that Shh expressed laterally **(e, f)** or dorsally **(g)** can induce Nkx2.1. **(h–k)** Staining for PLAP **(h)** demonstrated induction of the LGE-specific marker CRBP **(i)** by expression of Shh. See **(j)** for overlay. **(k)** Ectopic Shh expression dorsally (represented by PLAP, red) also induced CRBP in adjacent cells.

ous. Currently, we do not know how quickly this silencing occurs, or whether a silenced proviral insertion can subsequently resume expression.

We have demonstrated that vector expression in the ventricular zone of the telencephalon was substantially improved by using internal promoters. This suggests that the silencing is not an insurmountable property of most proviral insertions in this context, but rather is a function of the LTR as a regulatory element. The higher percentage of neurons labeled by CLC than by CLIA suggests that silencing was more prevalent among neuronal progenitors. However, we cannot rule out the possibility that unbiased silencing occurred in progenitors, and additional neuronal silencing occurred later in development. Although the EF1α and CA regulatory elements seem to overcome the proviral silencing, we cannot be sure that these elements were expressed with 100% reliability in all progenitors and subsequent cell types.

The vectors we describe here, in combination with ultrasound imaging, represent a significant advance over methods used in the past. Injection of E8.5 embryos resulted in widespread infection along the entire neural axis. Such infection events provide a means to introduce genes of interest into both the brain and spinal cord. Furthermore, the heavy infection observed in dorsal root ganglia suggests that this approach might be used to genetically modify the developing murine neural crest. In addition to infection of the nervous system, we saw infection in the skin, limbs, liver, heart and gut, suggesting that the method may have applications beyond the nervous system. As such, this system might also provide a testing ground for gene therapeutic approaches.

Ectopic expression of Shh *in utero*

Our interest in early patterning of the telencephalon led us to use the method presented here to examine the effects of ectopic Shh in this region. Shh has a central role in the dorsoventral patterning of the telencephalon, as is demonstrated by the finding that embryos lacking Shh do not develop ventral telencephalic structures[45]. Previous work from our lab and others has shown that explanted telencephalic tissue can be induced to express ventral markers, such as Nkx2.1 and Dlx-2, upon exposure to exogenous Shh protein[20,43]. These results are consistent with the loss-of-function phenotype, and the ability of Shh to ventralize more caudal neural tissue[38,40].

Although explants provide a powerful approach, they are limited by a short life span in culture, loss of cues from surrounding tissue and the tendency of tissue to become disorganized *in vitro*. Furthermore, because the brain undergoes major morphological changes between E8.5 and E10.5, and no clear fate map of the mouse forebrain exists, it is difficult to be certain of the normal fate of tissues placed in culture at different ages. Experiments conducted *in vivo*, however, retain embryonic context, and presumptive structures may be infected without detailed knowledge of what portions of the embryo will give rise to those structures.

As a first step toward analyzing the effect of Shh during telencephalic development *in vivo*, we infected embryos at E8.5 and E9.5 and assayed the expression of ventral markers at ectopic locations at E12.5. We found that Shh expressed in dorsal or lateral regions of the telencephalon can induce *dlx2*, Nkx2.1 and CRBP expression. As Nkx2.1 and CRBP are markers specific to the MGE and LGE, respectively, this result suggests that both structures can be induced by injection at E8.5. Further studies of this type, at both E8.5 and later ages, will allow us to examine *in vivo* the temporal change in responsiveness to Shh we have observed *in vitro*[20].

The spatial variability of retroviral infection will allow us to consider how different areas of the dorsal telencephalon respond to Shh. In some cases, for example, ectopic markers were not induced by Shh. Although there are several possible explanations for this result, one is that only certain regions are competent to respond to Shh at the time of infection. By combining the temporal versatility of this system with the random spatial locations of infection events, it should be possible to generate a spatio-temporal 'map' of the response of telencephalic tissue to Shh.

In the spinal cord, although we were able to locate many clusters of CLES-containing cells dorsally, we were unable to detect ectopic expression of the floor plate marker HNF3β (unpublished data). This lack of induction in the spinal cord may be because injection at E8.5 is too late, especially because the retrovirus is not likely to express much before E9.0–E9.5. This explanation is consistent with the finding that a transgene containing Shh driven dorsally by the Wnt-1 promoter does not induce HNF3β in the dorsal spinal cord[38]. We are currently looking for induction of other ventral markers such as Islet-1, and are exploring the possibility of injecting as early as E7.5–E8.0 in an effort to induce floor-plate markers in dorsal spinal cord. Nonetheless, this gain-of-function method presently can be used to examine the role of genes acting later in spinal cord development.

Future directions

The method presented here promises to be a powerful tool in the study of mammalian development, as it allows introduction of genes into numerous tissues at a wide variety of ages, without the need to identify suitable *cis*-acting regulatory elements. Because this method creates large clusters as well as isolated infected cells, it is well suited for studies addressing pattern formation, cell-fate specification, cellular differentiation and, ultimately, neuronal and glial function in the adult. Furthermore, it allows determination of whether candidate genes act cell-autonomously or nonautonomously.

Combination of this approach with mutant mouse strains may be particularly valuable. Such efforts would permit identification of those genes that are necessary for observed ectopic effects. For example, it will be interesting to see which, if any, of the *gli* genes—downstream effectors of Shh signaling[46]—are required for Shh to induce *dlx2*, Nkx2.1 and CRBP in the dorsal telencephalon. In general, such gain-of-function studies in mutant backgrounds will greatly facilitate the genetic dissection of pathways governing neural development in mammals.

Methods

Virus preparation. Because MLV/VSV viruses are pantropic and can infect human cells, all work with these viruses requires Biohazard Safety Level 2 containment practices. The production of MLV/VSV pseudotyped retroviral vectors has been described previously[22]. In short, the retroviral construct of choice was cotransfected into a 293-derived packaging cell line (293GP cells, Chiron, San Diego, California), along with pHCMV-G, which expresses the VSV-G protein. Cells were transfected at roughly 90% confluence using calcium phosphate precipitation in either 175-cm^2 flasks or 15-cm dishes. Each plate was transfected with 35 μg of pHCMV-G and 30 μg of the retroviral construct. Virus-containing supernatant was harvested and frozen at –80°C roughly 36, 48 and 60 hours after the start of transfection. Concentrated stocks were prepared by pooling the harvests, filtering them through a 0.45-μm filter, and pelleting for 1.5 hours in an SW28 rotor at 25,000 rpm at 4°C. Pellets were resuspended in 40 μl of PBS at 4°C for 4–12 h, and aliquots of virus were stored at –80°C. CLIA(E) was made in the same manner, although pHCMV-G was replaced with a construct expressing the ecotropic envelope.

Animals and surgery. All animals used in these studies were maintained according to protocols approved by the Institutional Animal Care and Use Committee at NYU School of Medicine. Timed-pregnant Swiss Webster mice used for injections were obtained from the Skirball Institute transgenic facility. The day on which the sperm plug was identified is referred to as E0.5. Animal care, preparation for surgery and the use of the ultrasound scanner (UBM scanner) have been described in detail elsewhere[19]. Viral stocks were diluted as desired with PBS, and Polybrene (Sigma) was added to a final concentration of 80 μg per ml. Approximately 1.0–1.5 μl of virus was injected into the telencephalic ventricle of E9.5 embryos or the amnionic cavity of E8.5 embryos. As exencephaly appears to be a byproduct of injection into the amnionic cavity at E8.5 (see Results), exencephalic embryos were not analyzed.

Sample preparation and analysis. Animals were killed by sodium pentobarbital overdose. Embryos were fixed by immersion in 4% paraformaldehyde (PFA) for 1–2 hours at 4°C, and P21 animals were transcardially perfused with 4% PFA and postfixed for 2–4 hours at 4°C. All samples were then sunk in 30% sucrose in PBS and embedded in HistoPrep (Fisher Scientific) on dry ice. Frozen sections were cut in a cryostat at 16–40 μm onto Colorfrost Plus slides (Fisher), were allowed to air dry and were stored at –20°C. Histochemical detection of PLAP was performed as follows: sections were first washed 3 × 5 min in PBS at room temperature, and then for 30 min in PBS preheated to 65°C. Following 5 min in PBS at room temperature, sections were placed in PLAP staining buffer (100 mM Tris-HCl, pH 9.5, 100 mM NaCl, 50 mM $MgCl_2$) for 5 min. Finally, 300 μl of staining solution (PLAP staining buffer containing nitroblue tetrazolium (NBT; 1 mg per ml) and 5-bromo-4-chloro-3-indolyl-phosphate (BCIP; 0.2 mg per ml)) were added to each slide and covered with a parafilm coverslip. Sections were stained for 36–40 hours at room temperature in the dark and were then washed with PBS for several hours. *In situ* hybridization to detect *dlx2* transcripts was done as described elsewhere[47].

Immunohistochemistry. The following antibodies were used for immunofluorescence: mouse anti-NeuN (1:100, Chemicon, Temecula, California), mouse anti-CNPase (1:150, Sternberger Monoclonals, Lutherville, Maryland), rabbit anti-GFAP (1:200, Accurate Chemical, Westbury, New York), sheep anti-PLAP (1:200, American Research Products, Belmont, Massachusetts), rabbit anti-PLAP (1:200, Accurate), rabbit anti-Nkx2.1 (1:300, Biopat Immunotechnologies, Caserta, Italy) and rabbit anti-CRBP (1:400, gift of U. Eriksson, Stockholm, Sweden). The following secondary antibodies were used: Cy3-conjugated donkey anti-sheep, FITC-conjugated donkey anti-rabbit, Cy3-conjugated goat anti-rabbit (all from Jackson ImmunoResearch, West Grove, Pennsylvania) and FITC-conjugated goat anti-mouse (Roche Molecular Biochemicals, Indianapolis, Indiana). Sections were washed in PBS, blocked for 1 h with PBS containing 10% donkey serum and 0.2% Triton X-100. Sections were incubated in primary antibodies diluted in block (with 1% or 10% serum) overnight at 4°C, then washed 3 times in PBS and incubated with secondary antibodies diluted in PBS containing 1% donkey serum and 0.2% Triton X-100 for 1–2 h at room temperature in the dark. Fluorescent images were obtained using either a cooled-CCD camera (Princeton Instruments) and Metamorph software (Universal Imaging, West Chester, Pennsylvania) or a confocal microscope (Leica).

Acknowledgements

We thank Rusty Lansford for bringing the CA regulatory element to our attention and Alex Langston and Robin Kimmel for input at the start of this work. We also thank Maria McCarthy and Connie Cepko for discussions, Michelle Starz-Gaiano for reading the manuscript, Ulf Eriksson for providing the anti-CRBP antibody and K. Mahon for the dlx2 in situ probe. This work was supported by NIH grants NS32993 (G.F.), NS38461 (D.H.T.) and HL62334 (D.H.T.). Additional support was provided by March of Dimes Grant 6-FY99-634 (G.F.). N.G. is supported by a postdoctoral fellowship from the American Cancer Society (PF4473).

Received 10 May; accepted 22 July 1999

1. Yan, Y. L., Jowett, T. & Postlethwait, J. H. Ectopic expression of hoxb2 after retinoic acid treatment or mRNA injection: disruption of hindbrain and craniofacial morphogenesis in zebrafish embryos. *Dev. Dyn.* **213**, 370–385 (1998).
2. Gaiano, N. & Hopkins, N. Introducing genes into zebrafish. *Biochim. Biophys. Acta.* **1288**, O11–14 (1996).
3. Slack, J. M. Inducing factors in Xenopus early embryos. *Curr. Biol.* **4**, 116–126 (1994).
4. Bell, E. J. & Brickell, P. M. Replication-competent retroviral vectors for expressing genes in avian cells in vitro and in vivo. *Mol. Biotechnol.* **7**, 289–298 (1997).
5. Muramatsu, T., Mizutani, Y., Ohmori, Y. & Okumura, J. Comparison of three nonviral transfection methods for foreign gene expression in early chicken embryos in ovo. *Biochem. Biophys. Res. Commun.* **230**, 376–380 (1997).
6. Davidson, B. L., Allen, E. D., Kozarsky, K. F., Wilson, J. M. & Roessler, B. J. A model system for in vivo gene transfer into the central nervous system using an adenoviral vector. *Nat. Genet.* **3**, 219–223 (1993).
7. Moriyoshi, K., Richards, L. J., Akazawa, C., O'Leary, D. D. & Nakanishi, S. Labeling neural cells using adenoviral gene transfer of membrane-targeted GFP. *Neuron* **16**, 255–260 (1996).
8. Price, J., Turner, D. & Cepko, C. Lineage analysis in the vertebrate nervous system by retrovirus-mediated gene transfer. *Proc. Natl. Acad. Sci. USA* **84**, 156–160 (1987).
9. Sanes, J. R., Rubenstein, J. L. & Nicolas, J. F. Use of a recombinant retrovirus to study post-implantation cell lineage in mouse embryos. *EMBO J.* **5**, 3133–3142 (1986).
10. Roe, T., Reynolds, T. C., Yu, G. & Brown, P. O. Integration of murine leukemia virus DNA depends on mitosis. *EMBO J.* **12**, 2099–2108 (1993).
11. Cepko, C. L., Fields-Berry, S., Ryder, E., Austin, C. & Golden, J. Lineage analysis using retroviral vectors. *Curr. Top. Dev. Biol.* **36**, 51–74 (1998).
12. Turner, D. L. & Cepko, C. L. A common progenitor for neurons and glia persists in rat retina late in development. *Nature* **328**, 131–136 (1987).
13. Walsh, C. & Cepko, C. L. Widespread dispersion of neuronal clones across

functional regions of the cerebral cortex. *Science* **255**, 434–440 (1992).
14. Furukawa, T., Morrow, E. M. & Cepko, C. L. Crx, a novel otx-like homeobox gene, shows photoreceptor-specific expression and regulates photoreceptor differentiation. *Cell* **91**, 531–541 (1997).
15. Ishibashi, M. *et al.* Persistent expression of helix-loop-helix factor HES-1 prevents mammalian neural differentiation in the central nervous system. *EMBO J.* **13**, 1799–1805 (1994).
16. Burrows, R. C., Wancio, D., Levitt, P. & Lillien, L. Response diversity and the timing of progenitor cell maturation are regulated by developmental changes in EGFR expression in the cortex. *Neuron* **19**, 251–267 (1997).
17. Bao, Z. Z. & Cepko, C. L. The expression and function of Notch pathway genes in the developing rat eye. *J. Neurosci.* **17**, 1425–1434 (1997).
18. Olsson, M., Campbell, K. & Turnbull, D. H. Specification of mouse telencephalic and mid-hindbrain progenitors following heterotopic ultrasound-guided embryonic transplantation. *Neuron* **19**, 761–772 (1997).
19. Liu, A., Joyner, A. L. & Turnbull, D. H. Alteration of limb and brain patterning in early mouse embryos by ultrasound-guided injection of Shh-expressing cells. *Mech. Dev.* **75**, 107–115 (1998).
20. Kohtz, J. D., Baker, D. P., Corte, G. & Fishell, G. Regionalization within the mammalian telencephalon is mediated by changes in responsiveness to Sonic Hedgehog. *Development* **125**, 5079–5089 (1998).
21. Naviaux, R. K., Costanzi, E., Haas, M. & Verma, I. M. The pCL vector system: rapid production of helper-free, high-titer, recombinant retroviruses. *J. Virol.* **70**, 5701–5705 (1996).
22. Yee, J. K., Friedmann, T. & Burns, J. C. Generation of high-titer pseudotyped retroviral vectors with very broad host range. *Methods Cell Biol.* **43**, 99–112 (1994).
23. Eidelman, O., Schlegel, R., Tralka, T. S. & Blumenthal, R. pH-dependent fusion induced by vesicular stomatitis virus glycoprotein reconstituted into phospholipid vesicles. *J. Biol. Chem.* **259**, 4622–4628 (1984).
24. Albritton, L. M., Tseng, L., Scadden, D. & Cunningham, J. M. A putative murine ecotropic retrovirus receptor gene encodes a multiple membrane-spanning protein and confers susceptibility to virus infection. *Cell* **57**, 659–666 (1989).
25. Lange, C. & Blankenstein, T. Loss of retroviral gene expression in bone marrow reconstituted mice correlates with down-regulation of gene expression in long-term culture initiating cells. *Gene Ther.* **4**, 303–308 (1997).
26. Gorman, C. M., Rigby, P. W. & Lane, D. P. Negative regulation of viral enhancers in undifferentiated embryonic stem cells. *Cell* **42**, 519–526 (1985).
27. Kempler, G., Freitag, B., Berwin, B., Nanassy, O. & Barklis, E. Characterization of the Moloney murine leukemia virus stem cell-specific repressor binding site. *Virology* **193**, 690–699 (1993).
28. Johansson, C. B. *et al.* Identification of a neural stem cell in the adult mammalian central nervous system. *Cell* **96**, 25–34 (1999).
29. Temple, S. & Alvarez-Buylla, A. Stem cells in the adult mammalian central nervous system. *Curr. Opin. Neurobiol.* **9**, 135–141 (1999).
30. Reynolds, B.A. & Weiss, S. Clonal and population analyses demonstrate that an EGF-responsive mammalian embryonic CNS precursor is a stem cell. *Dev. Biol.* **175**, 1–13 (1996).
31. Halliday, A. L. & Cepko, C. L. Generation and migration of cells in the developing striatum. *Neuron* **9**, 15–26 (1992).
32. Takahashi, T., Nowakowski, R. S. & Caviness, V. S. Jr. The leaving or Q fraction of the murine cerebral proliferative epithelium: a general model of neocortical neuronogenesis. *J. Neurosci.* **16**, 6183–6196 (1996).
33. Johnson, A. D. & Krieg, P. A. pXeX, a vector for efficient expression of cloned sequences in Xenopus embryos. *Gene* **147**, 223–226 (1994).
34. Sawicki, J. A., Morris, R. J., Monks, B., Sakai, K. & Miyazaki, J. A composite CMV-IE enhancer/beta-actin promoter is ubiquitously expressed in mouse cutaneous epithelium. *Exp. Cell Res.* **244**, 367–369 (1998).
35. Niwa, H., Yamamura, K. & Miyazaki, J. Efficient selection for high-expression transfectants with a novel eukaryotic vector. *Gene* **108**, 193–199 (1991).
36. Tan, S. S. & Breen, S. Radial mosaicism and tangential cell dispersion both contribute to mouse neocortical development. *Nature* **362**, 638–640 (1993).
37. Rakic, P. Radial versus tangential migration of neuronal clones in the developing cerebral cortex. *Proc. Natl. Acad. Sci. USA* **92**, 11323–11327 (1995).
38. Echelard, Y. *et al.* Sonic hedgehog, a member of a family of putative signaling molecules, is implicated in the regulation of CNS polarity. *Cell* **75**, 1417–1430 (1993).
39. Ericson, J. *et al.* Sonic hedgehog induces the differentiation of ventral forebrain neurons: a common signal for ventral patterning within the neural tube. *Cell* **81**, 747–756 (1995).
40. Roelink, H. *et al.* Floor plate and motor neuron induction by vhh-1, a vertebrate homolog of hedgehog expressed by the notochord. *Cell* **76**, 761–775 (1994).
41. Bulfone, A. *et al.* The mouse Dlx-2 (Tes-1) gene is expressed in spatially restricted domains of the forebrain, face and limbs in midgestation mouse embryos. *Mech. Dev.* **40**, 129–140 (1993).
42. Lazzaro, D., Price, M., de Felice, M. & Di Lauro, R. The transcription factor TTF-1 is expressed at the onset of thyroid and lung morphogenesis and in restricted regions of the foetal brain. *Development* **113**, 1093–1104 (1991).
43. Shimamura, K. & Rubenstein, J. L. Inductive interactions direct early regionalization of the mouse forebrain. *Development* **124**, 2709–2718 (1997).
44. Toresson, H., Mata de Urquiza, A., Fagerstrom, C., Perlmann, T. & Campbell, K. Retinoids are produced by glia in the lateral ganglionic eminence and regulate striatal neuron differentiation. *Development* **126**, 1317–1326 (1999).
45. Chiang, C. *et al.* Cyclopia and defective axial patterning in mice lacking Sonic hedgehog gene function. *Nature* **383**, 407–413 (1996).
46. Ruiz i Altaba, A. Catching a Gli-mpse of Hedgehog. *Cell* **90**, 193–196 (1997).
47. Schaeren-Wiemers, N. & Gerfin-Moser, A. A single protocol to detect transcripts of various types and expression levels in neural tissue and cultured cells: in situ hybridization using digoxigenin-labelled cRNA probes. *Histochemistry* **100**, 431–440 (1993).
48. Mullen, R. J., Buck, C. R. & Smith, A. M. NeuN, a neuronal specific nuclear protein in vertebrates. *Development* **116**, 201–211 (1992).
49. Sprinkle, T. J. 2',3′-cyclic nucleotide 3′-phosphodiesterase, an oligodendrocyte-Schwann cell and myelin-associated enzyme of the nervous system. *Crit. Rev. Neurobiol.* **4**, 235–301 (1989).
50. Bignami, A. & Dahl, D. Astrocyte-specific protein and neuroglial differentiation. An immunofluorescence study with antibodies to the glial fibrillary acidic protein. *J. Comp. Neurol.* **153**, 27–38 (1974).